Predicting the Enantioseparation Efficiency of Chiral Mandelic Acid in Diastereomeric Crystallization Using a Quartz Crystal Microbalance

ARTICLE *in* CRYSTAL GROWTH & DESIGN · DECEMBER 2010

Impact Factor: 4.89 · DOI: 10.1021/cg100275v

5 AUTHORS, INCLUDING:

Jong-Min Kim
Dong-A University
120 PUBLICATIONS **726** CITATIONS
SEE PROFILE

Xuan-Hung Pham
Konkuk University
25 PUBLICATIONS **282** CITATIONS
SEE PROFILE

DOI: 10.1021/cg100275v

CRYSTAL GROWTH & DESIGN Article

2011, Vol. 11
53–58

Predicting the Enantioseparation Efficiency of Chiral Mandelic Acid in Diastereomeric Crystallization Using a Quartz Crystal Microbalance

Hui-Shi Guo,[†,⊥] Jong-Min Kim,[‡] Xuan-Hung Pham,[§] Sang-Mok Chang,[‡] and Woo-Sik Kim*[,§]

[†]*Department of Chemistry, Shaoguan University, Shaoguan 512005, PR China,* [‡]*Department of Chemical Engineering, Dong A University, Busan 604-714, Korea, and* [§]*Department of Chemical Engineering, Kyung Hee University, Kyungki-do 446-701, Korea.* [⊥]*Current address: Kyung Hee University. E-mail: guohuishi@163.com.*

Received March 1, 2010; Revised Manuscript Received November 7, 2010

ABSTRACT: This study uses quartz crystal microbalance (QCM) chiral recognition as a novel approach to predict the chiral recognizability of a chiral selector for a racemate. The chiral selector (L-phenylalanine, L-Phe) was immobilized on a QCM sensor surface using a two-step assembly procedure. The modification of the L-Phe on the sensor surface was then characterized using several techniques, including resonant frequency detection, the contact angle, and X-ray photoelectron spectroscopy measurements. When examining the chiral recognizability of the L-Phe-modified QCM sensor for L-mandelic acid (L-MA) using a vapor diffused molecular assembly reaction technique, the chiral discrimination factor between L- and D-MA was about 8. The practical diastereomeric crystallization resolution of a MA racemic compound was then carried out using L-Phe as the resolving agent. The different properties of the diastereomer crystals of L-Phe-L-MA and L-Phe-D-MA were confirmed using high performance liquid chromatography (HPLC) and differential scanning calorimetry (DSC) analysis, plus the factors influencing the chiral resolution, such as molar ratio of MA to L-Phe, agitation speed, pH, cooling rate, and crystallization temperature were examined. The results showed that the diastereomeric crystallization separation of racemate MA using L-Phe as the resolving agent matched well with the QCM chiral recognition results. Therefore, the proposed method using QCM chiral recognition offers a simple solution to the challenge of screening a resolving agent for diastereomeric crystallization.

1. Introduction

Enantiomers can have very different physiological effects on human beings, where one can exhibit desirable physiological, pharmacological, pharmacodynamic, and pharmacokinetic properties, while the other can exhibit toxicity toward living organisms and different activities in chemical and biotechnological processes.[1−3] Although the majority of commercially available drugs are now both synthetic and chiral, a large number of chiral drugs are still marketed as racemates. Thus, to avoid possible undesirable side effects from chiral drugs, more methods for separating chiral compounds are urgently needed.

Among the various methods that have already been developed to prepare chiral compounds,[4−6] diastereomeric crystallization is one of the most popular practical techniques used in the industry due to its relative simplicity, low cost, and use of standard production equipment.[7−11] Thus, most companies try using diastereomeric crystallization first, and only use other methods if it does not work. The principle of diastereomeric crystallization is based on the formation of diastereomeric salts from a racemate using an optically pure compound (resolving agent). Since the two resulting diastereomers have different physicochemical properties, one can then be selectively crystallized through traditional techniques. This chiral resolution technique is traditionally used for the separation of racemic mandelic acid (MA),[12−14] which provides important chiral analogues that are widely employed in the synthesis of various products, such as penicillin, cephalosporin, antiobesity medicine, and some other pharmaceuticals.[15−17]

Recently, a new approach to the resolution of racemate, named as "Dutch Resolution", was introduced, which was an effective method to determine the resolving agent for the chiral resolution.[18−20] On the basis of combinatorial chemistry, in this approach, the family of the resolving agents was designed and applied to the classical resolutions, resulting in a significantly high success rate compared to the convention resolution method.[21] There was a most common family of the resolving agents derived from cyclic phosphoric acid by ten Hoeve and Wynberg.[22,23] As an example, Loh et et al applied a derivative family, the (−)-ephidrine-cyclic phosphoric acid system, for the chiral resolution and investigation of its mechanism.[24]

A quartz crystal microbalance (QCM) is a newly developed molecular recognition technique that is remarkably sensitive to mass and inexpensive in analytical applications.[25−29] However, molecular recognition using the QCM in the liquid phase is inherently difficult, as it is much more difficult to achieve a sufficiently stable resonance signal in the liquid phase than in the gas phase for two main reasons: the dense and viscous medium of the liquid phase and the tight mechanical sealing of liquid cell.[30,31] In our previous studies, a new QCM technique, called vapor diffused molecular assembly (VDMA) method, was successfully developed for sensing the molecular recognition in the gas phase.[32−34] For the chiral recognition using a QCM, selecting a chiral selector and building it on the sensor surface is most critical.[35−39]

Therefore, in the present study it is attempted to demonstrate the applicability of a novel approach using a QCM for the prediction of resolving agent (L-phenylalanine, L-Phe) and the quantitative evaluation of its molecular recognizability for the chiral separation (mandelic acid, MA). Subsequent practical

*Corresponding author. E-mail: wskim@khu.ac.kr. Phone: +82-31-201-2970. Fax: +82-31-273-2971.

Published on Web 12/03/2010

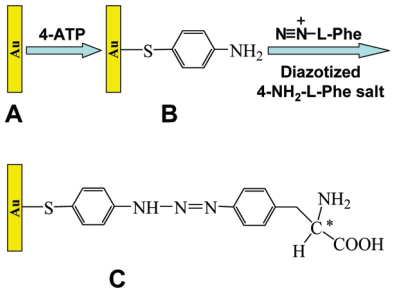

Figure 1. Schematic representation of fabrication process of L-Phe-modified sensor. (A) Bare QCM sensor surface, (B) ATP-SAMs-coated QCM sensor surface, and (C) L-Phe-modified QCM sensor surface.

diastereomeric crystallization resolution of a MA racemic compound using L-Phe as the resolving agent confirms the prediction. This would appear to be the first report on the use of QCM chiral sensing to select and evaluate a resolving agent for diastereomeric crystallization.

2. Experimental Section

2.1. Materials and Reagents. L-Mandelic acid (L-MA), D-mandelic acid (D-MA), 4-aminothiophenol (ATP), *p*-amino-L-phenylalanine hydrochloride (4-NH_2-L-Phe), potassium dihydrogen phosphate/disodium hydrogen phosphate buffer (pH 7.0) were purchased from Sigma-Aldrich (ACS grade, U.S.A.). All the other reagents were commercially available and of analytical reagent grade. Deionized water was used throughout all the experiments.

2.2. Apparatus. The QCM measurements were carried out using AT-cut quartz crystals with gold electrodes (areas, 0.2 cm^2) and a resonant frequency of 9 MHz (Seiko EG&G, Chiba, Japan). All the QCM responses were measured in a constant-temperature oven (25 °C) under N_2 atmosphere conditions using QCM 922 (Princeton Applied Research, USA). The mass change recorded by the QCM sensor was calculated according to the Sauerbrey equation.[40] The water contact angle was measured using a Phoenix 300 contact angle meter (Surface Electro Optics Co., Korea). The X-ray photoelectron spectroscopy (XPS) was performed using a K-Alpha XPS spectrometer (Thermo Electric Company). A monochromated Al anode (Al Kα radiation line: 1486.6 eV) was used as the X-ray source. The HPLC analysis was conducted using an Agilent 1100 series HPLC (Agilent, U.S.A.) with a UV detector at a 254 nm wavelength. A Pickle Covalent (S,S) Whelk-01 reverse column (250 mm × 4.6 mm) was used to analyze the molar ratio composition of mandelic acids and the resolving agent in the diastereomers, and an aqueous solution of 1.0% (v/v) acetic acid at a flow rate of 1 mL/min used as the mobile phase. In addition, a Kromasil 100-5-TBB column (250 mm × 4.6 mm) was used to analyze the enantiomer purity in the diastereomers based on a mixture of hexane, *tert*-butyl methyl ether, and formic acid at a ratio of 75.0, 24.5, and 0.5% (v/v), respectively, as the mobile phase, also with a flow rate of 1 mL/min. The melting point and enthalpy change of the diastereomeric crystals were measured using a photocalorimeter (DSC Q100 system, U.S.A.). Samples of the diastereomeric crystals air-tightly sealed in aluminum pans were thermally scanned from 300 to 573 K at a heating rate of 5 K/min under a nitrogen atmosphere (nitrogen flow rate of 50 mL/min).

2.3. Immobilization of Chiral Selectors on QCM Sensors. A schematic representation of the preparation process of the L-Phe-modified QCM sensor is shown in Figure 1, which consists of two steps.

First, the gold films of the QCM sensors were cleaned by dipping them in a Piranha solution (3:1 H_2SO_4/30% H_2O_2, Caution: this is highly oxidative for organic compounds and should only be used with protection) at room temperature for 30 s immediately before use, followed by copious rinsing with water. The sensors were then washed thoroughly with acetone and absolute ethanol, and finally dried with purified N_2. Next, the cleaned sensors were immediately immersed in a 1 mM solution of ATP in absolute ethanol at 4 °C for 24 h to form a self-assembled monolayer (SAM). Thereafter, the sensors were rinsed and sonicated with absolute ethanol to remove any physically adsorbed molecules.

A diazotization coupling reaction was then used to couple the 4-NH_2-L-Phe to the sensor-immobilized ATP, thereby preserving both the α-amino and carboxyl groups attached to the stereogenic center.[41] For this purpose, 4-NH_2-L-Phe at a concentration of 5.6 mg/mL was dissolved in 0.2 M HCl and subsequently mixed with $NaNO_2$ (35 mg/mL) at a ratio of 1:9 (v/v) for 1 h at 0 °C. The resulting solution was then added dropwise to the ATP-modified sensor immersed in a potassium dihydrogen phosphate/disodium hydrogen phosphate buffer (pH 7.0). The sensors were finally washed with absolute ethanol and dried with purified N_2.

2.4. Chiral Recognition of Mandelic Acid on L-Phe-Modified QCM Sensor. The chiral recognition reaction was performed using a vapor diffused molecular assembly (VDMA) reaction approach, as described elsewhere.[32,33] Before the sensing, the frequency of the modified QCM sensor (F_1) was detected in a detection chamber under N_2 atmosphere conditions at 25 °C. The modified QCM sensor was then fixed in the 100 mL reaction chamber that was placed in an oven with a constant temperature of 25 °C. Next, 1 mL of the reaction solution was carefully injected into the reaction container while maintaining a VDMA reaction for a certain time period. Finally, the sensor was moved out and the resonant frequency was detected again (F_2). The frequency change (ΔF), calculated as $\Delta F = F_2 - F_1$, reflects the material mass that attached to the sensor during the VDMA reaction period.

2.5. Diastereomeric Crystallization. The diastereomeric crystallization separation of D/L-MA (racemate) using L-Phe as the resolving agent was carried out in a 50-mL double-jacketed Ruston reactor. First, a fixed amount (0.600 g) of L-Phe was dissolved in a series of 10-mL racemic MA solutions with various racemic concentrations ranging from 0.145−2.171 mol/L to meet a molar ratio of D/L-MA to L-Phe from 0.4 to 8.0, and then heated up to 80 °C for complete dissolution. Thereafter, the clear solution was cooled down to induce diastereomeric crystallization, and left for 2 h. The crystallization temperature was changed from 25 to 60 °C and the cooling rate was varied from 10 to 60 °C/h. The crystal product was then filtrated out through a 0.45 μm micromembrane filter, dried in an oven at room temperature, and analyzed with regard to the diastereomeric resolution, structure, and thermal properties of the crystals.

3. Results and Discussion

3.1. Characterization of L-Phe-Modified QCM Sensors. To monitor the changes on the gold surface during the modification process, several techniques were used to characterize the surface after each modification step, as follows.

The resonant frequency changes of the QCM sensors were detected using the QCM measurements, while the mass changes were calculated according to the Sauerbrey equation[31] after the stepwise modification of the sensor surface. The frequency of the QCM sensor after the ATP immobilization decreased 32.3 Hz, corresponding to 33.9 ng of ATPs loaded on the sensor surface and a surface coverage, Γ_{QCM}, of 6.8×10^{-10} mol/cm^2. Further modifications with 4-NH_2-L-Phe resulted in a frequency decrease of 112.7 Hz, corresponding to 118.3 ng (i.e., 0.62 nmol) of materials loaded on the sensor surface. Thus, the frequency decrease and mass increase with both fabrication steps, as determined by the QCM, confirmed the stepwise formation of the ATP and L-Phe layers on the sensor surface.

The contact angle is an important surface characteristic; thus a change in the contact angle is direct evidence of surface modification. The bare QCM sensor surface exhibited a low hydrophilicity with a contact angle of 88.2°. However, after the ATP modification, the contact angle decreased to 70.3°, indicating an increase in the hydrophilicity of the surface, due to the hydrophilic property of the amino end-group of ATP.

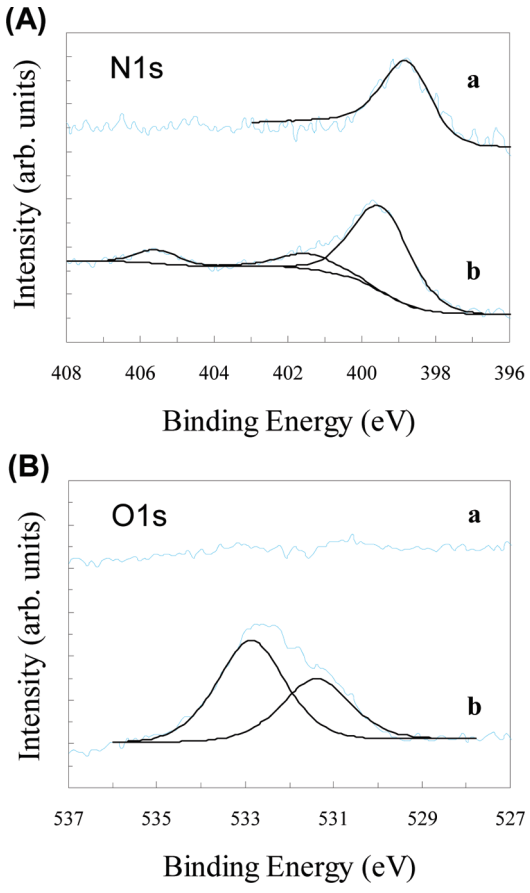

Figure 2. XPS spectrum of ATP-SAMs-coated QCM sensor (a) and L-Phe-modified QCM sensor (b) with unmodified QCM sensor as background reference. (A) N 1s region and (B) O 1s region.

Further modifications with 4-NH_2-L-Phe only produced a slight change in the hydrophilicity of the surface, as the contact angle changed to 68.6°.

The O 1s and N 1s spectra were also recorded to provide evidence of the stepwise modification of the gold sensor surface, with an unmodified QCM sensor as the background reference (Figure 2). As seen, the N 1s spectrum of the ATP-coated QCM sensor (Figure 2A, curve a) showed a peak at 399.4 eV that was attributed to the $-NH_2$ end group of the immobilized ATP.[42,43] After the L-Phe modification, two new peaks appeared at 401.3 and 405.3 eV (Figure 2A, curve b). According to the modification scheme shown in Figure 1, these two new peaks may correspond to the nitrogen atoms in the $-NH—N{=}N-$ structure. Meanwhile, the O 1s spectrum of the ATP-modified surface did not show any peaks (Figure 2B, curve a) due to the absence of oxygen atoms in ATP. After the L-Phe modification, a new peak appeared at 531.1 eV (Figure 2B, curve b), which was assigned to the oxygen atoms in the carboxyl group of L-Phe.[43,44]

All the resonant frequency detection, contact angle, and XPS detection results presented above confirmed the successful modification of L-Phe on the sensor surface.

3.2. Chiral Recognizability of L-Phe-Modified QCM Sensor to Chiral Mandelic Acid. The chiral recognizability of the L-Phe-modified QCM sensor for chiral mandelic acid was investigated by QCM frequency detection using the VDMA method, as described in section 2.4.

Figure 3 shows a plot of the frequency changes of the L-Phe-modified sensor (ΔF) versus the VDMA reaction time

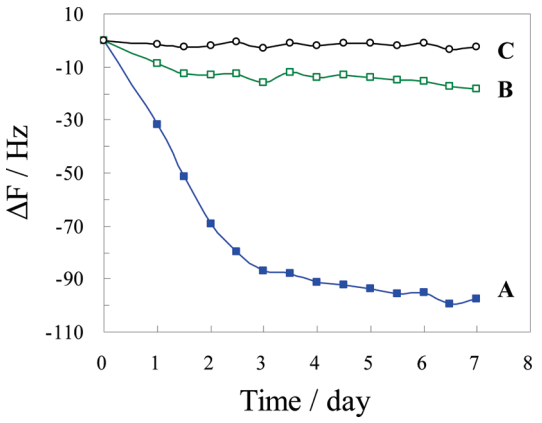

Figure 3. Frequency change of L-Phe-modified QCM sensor after VDMA reaction with (A) 1 mL of 0.05 mol/L L-mandelic acid, (B) 1 mL of 0.05 mol/L D-mandelic acid, and (C) 1 mL of deionized H_2O for different time periods at 25 °C. The volume of the reaction chamber was 100 mL, the detecting temperature was controlled at 25 °C, and the detection was performed under N_2 atmosphere conditions.

with respect to the chiral mandelic acid (L-MA and D-MA) and deionized water. As shown in the figure, the frequency response of the modified QCM sensor to L-MA decreased almost linearly for the first 2.5 days (curve A), indicating that before the VDMA equilibrium was reached, a longer reaction time allowed more L-MA molecules to attach to the sensor surface and larger frequency changes. After a specific VDMA period (≥3 days), the frequency changes tended to level off, indicating that the reaction equilibrium was achieved. After a VDMA reaction period of 7 days, the frequency change was found to be 95.0 Hz, corresponding to 99.8 ng (i.e., 0.66 nmol) of L-MA attached to the L-Phe-modified QCM sensor surface and a molecular binding ratio of sensor-immobilized L-Phe to L-MA of about 1:1.[45]

To confirm that the observed frequency changes were indeed based on the specific interaction between the sensor-immobilized L-Phe and the L-MA, a further blank experiment with deionized H_2O and control experiment with D-MA were performed. As shown by curve C, no distinct frequency changes were detected with the deionized H_2O. Meanwhile, for the D-MA, the frequency response of the modified QCM sensor decreased a little (about 11 Hz) during the first 2 days, and then became almost stable after 2.5 days or more (curve B), indicating that only a very small amount of D-MA was attached to the modified sensor surface.

Therefore, these results indicate that the frequency changes observed with L-MA were due to specific host−guest interactions rather than nonspecific adsorption, and that the L-Phe-modified sensor surface had a selective chiral recognition ability for chiral mandelic acid. The chiral discrimination factor between L and D-MA, $\alpha_{\text{L-MA/D-MA}} = \Delta F_{\text{L-MA}}/\Delta F_{\text{D-MA}}$, was found to be about 8, suggesting that L-Phe can be good resolving agent for the diastereomeric crystallization separation of L-MA.

3.3. Characterization of the Diastereomer. On the basis of the QCM chiral recognition results, diastereomeric crystallization separation of L-MA from a racemic compound was carried out using L-phenylalanine as the resolving agent. As shown in Figure 4, the solubility of L-Phe-L-MA was much lower than that of L-Phe-D-MA, implicitly indicating the stronger interaction between L-Phe and L-MA than between L-Phe and D-MA. According to the crystallographic

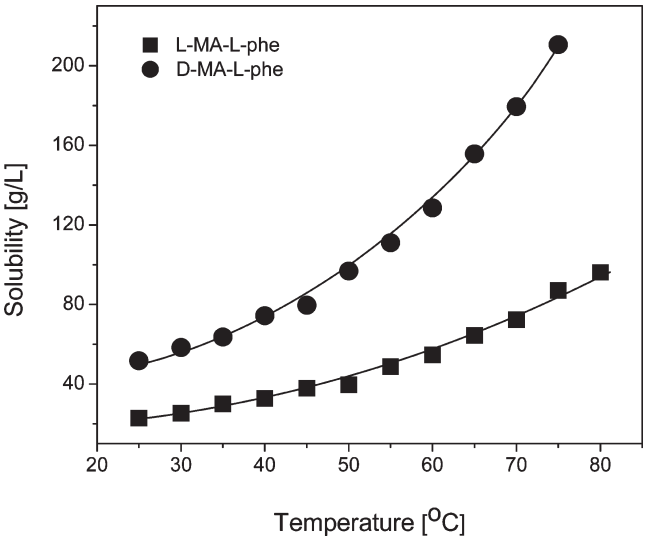

Figure 4. Solubility of diastereomer crystals depending on temperature.

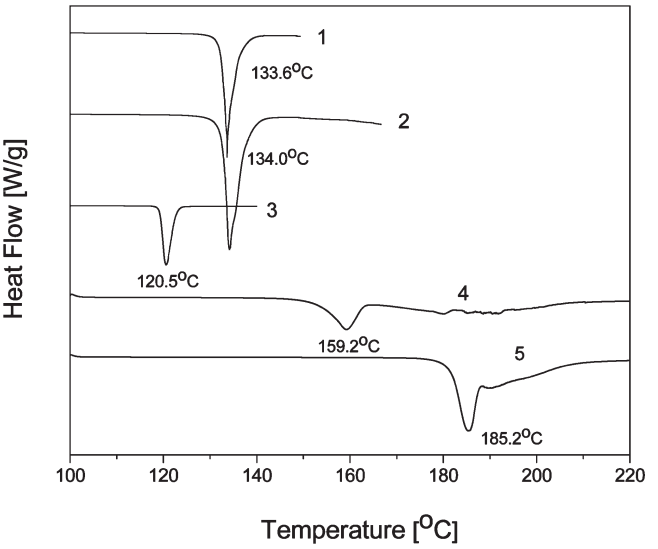

Figure 5. Thermal analysis of (1) L-MA crystals, (2) D-MA crystals, (3) D/L-racemic crystals, (4) L-Phe-D-MA crystals, (5) L-Phe-L-MA crystals.

investigation of diastereomeric crystals, a common characteristic hydrogen-bond network was formed in L-Phe-L-MA crystals.[46] Two pair of mandelate anions and primary ammonium cations in a unit, where the pairs were related to each other by a 2-fold screw axis, constructed three kinds of hydrogen bonds between the carboxylate oxygens and the three ammonium hydrogens. In addition, the carboxylate anion of both L-phenylalanine and L-MA has generated two hydrogen bonds. Each unit has hydrogen bonds with translational neighboring units, resulting in the formation of an infinite columnar structure (2_1-column) which is stable and favorable from the viewpoint of hydrogen bonding interaction. The structure is frequently found in the crystal structures of the salts of ammonium cations with carboxylate anions.[47,48]

Meanwhile, in the diastereomer of L-Phe-D-MA, the stable 2_1-column hydrogen bond pattern by carboxylate and ammonium was not found. It had six kinds of hydrogen bonds but two out of them were bifurcated hydrogen bonds reducing the interaction force of its hydrogen bond. Thus, the lattice energy as well as interaction forces of L-Phe-D-MA were lower than that of L-Phe-L-MA, resulting in the higher solubility. It consistently agreed with the above solubility data of the two diastereomers and would be the reason why the L-Phe was preferentially combined with the L-MA and crystallized out first as diastereomeric crystals of L-Phe-L-MA.

Such characteristic of the diastereomers could be confirmed by the thermal analysis of DSC, as shown in Figure 5. The melting points of two enantiomers of L- and D-MA were almost identical at about 134 °C, and their racemate of D/L-MA melted at 120 °C. However, the melting points of two diastereomers were much high at 185.2 °C for L-Phe-L-MA and 159.2 °C for L-Phe-D-MA, respectively, indicating that the L-Phe-L-MA diastereomer possessed a higher thermal stability and more lattice energy than the L-Phe-D-MA diastereomer due to the stronger hydrogen bonding in the L-Phe-L-MA crystal structure when compared to the L-Phe-D-MA crystal structure.[45] In addition, when considering the melting point of L-phenylalanine at about 230 °C, those DSC results indicated that the L-MA was more thermally stabilized by the diastereomerization with the-L-Phe than the D-MA and dissociated at the high temperature of 185.2 °C. It should be noticed that from DSC and TGA analysis, the enantiomer L- and D-MA were decomposed at around 140−150 °C after melting. Thus, the broad thermal peaks of two diastereomers might be due to the simultaneous decomposition of MA after melting.

3.4. Diastereomeric Crystallization Parameters. The several operating factors influencing the chiral resolution were also investigated through a series of single factor experiments. According to our previous study, it was found that the molar ratio of racemic MA to L-Phe ($R_{MA/L\text{-}Phe}$) was a critical factor in the formation of diastereomers. Within a molar ratio range $R_{MA/L\text{-}Phe}$ of 0.7−5.0, crystals were obtained with a 1:1 molecular ratio of MA to L-Phe, implying a diastereomer, and the diastereomeric excess of the crystals was enhanced from 50 to 70% when increasing the molar ratio. However, the recovery of L-MA by the diastereomeric crystallization was maximized as 46.3% at an $R_{MA/L\text{-}Phe}$ of 2.0 and then reduced as 24.3% as further increasing $R_{MA/L\text{-}Phe}$ to 5.0. Thus, in the present study, an $R_{MA/L\text{-}Phe}$ of 2.0 was fixed as the optimal molar ratio for the further diastereomeric crystallization.

There were many attempts to consider the influence of agitation speed on the chiral nucleation.[49−51] As shown in Figure 6, the diastereomeric excess of the crystals was proportionally enhanced from 53% to 63% with agitation speed until 500 rpm and then slightly increased to 64% by a further increase of the agitation speed up to 1000 rpm. According to the Veintemillas-Verdaguer et al.'s study of chiral crystallization, the enantiomer resolution increased with the agitation speed due to the depression of the heterogeneous surface nucleation and incorporation of the opposite enantiomer.[52] Thereby, it might be guessed that the higher agitation speed inhibited the diastereomerization of D-MA with L-Phe and its incorporation into crystals, resulting in the higher diastereomeric excess of the crystals. In addition, the secondary nucleation of the L-Phe-L-MA was promoted by the agitation, contributing to the increase of the diastereomeric excess with agitation speed.[49]

The influence of pH on the diastereomeric crystallization was investigated, as shown in Figure 7. It was already known

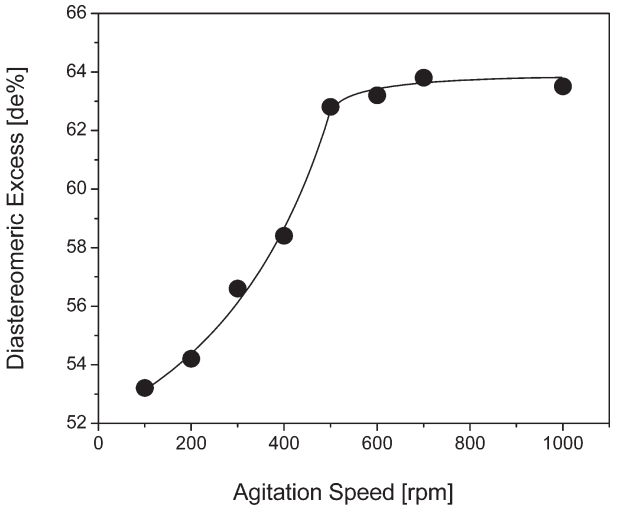

Figure 6. Effect of agitation speed on diastereomeric excess of enantio-separation. The molar ratio of MA to L-Phe = 2.0, pH = 3.0, cooling rate = 10 °C/h, crystallization temperature = 30 °C.

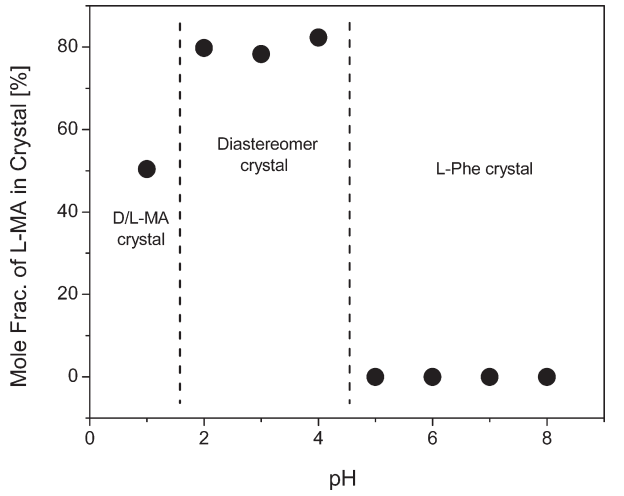

Figure 7. Effect of solution pH on diastereomeric resolution for enantio-separation. Here, *y*-axis "Mole Fraction of L-MA in Crystal" meant the molar fraction of L-MA between D/L-MA contained in crystals obtained from crystallization. The molar ratio of MA to L-Phe = 2.0, agitation speed = 500 rpm, cooling rate = 10 °C/h, crystallization temperature = 30 °C.

that charges of L-Phe and MA varied with solution pH, as below:

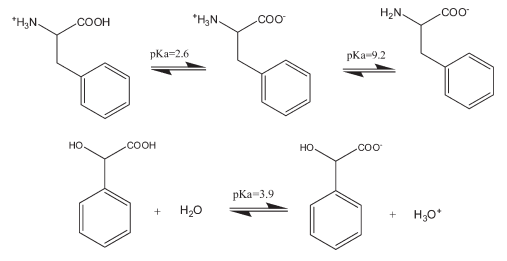

That is, at a solution pH higher than 5.0, L-Phe and MA were charged as the anion due to the deprotonation of carboxyl group (COO^-). It was a repulsive force between the negative-charged COO^-s in both molecules. Therefore, they were hardly diastereomerized nor crystallized out in solution. Here, it should be mentioned that at pH above 5.0, the L-Phe was crystallized out alone because the L-Phe was neutral in charge and its solubility was minimized.

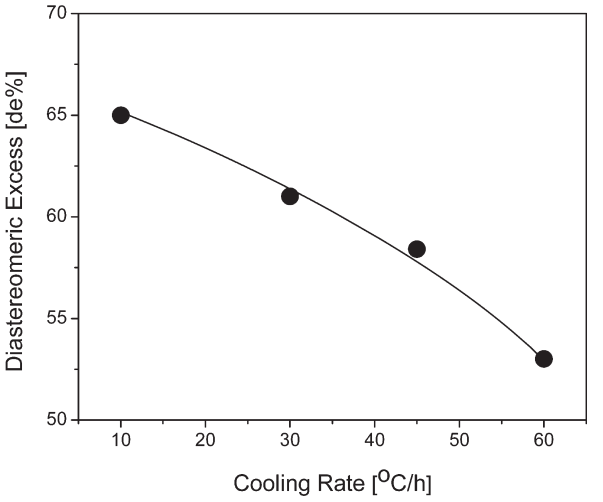

Figure 8. Effect of cooling rate on diastereomeric excess of enantio-separation. The molar ratio of MA to L-Phe = 2.0, pH = 3.0, agitation speed = 500 rpm, crystallization temperature = 30 °C.

At a solution pH lower than 2.0, the interaction between the L-Phe and MA broke down due to the formation of L-Phe hydrochloride salts, crystallizing out the racemate of MA alone. Therefore, a pH range of 2.0−4.0 was selected, where most of the L-phenylalanine molecules existed as zwitterions, while the MA showed a neutral charge. This also meant that the two molecules had almost no electrostatics, thereby allowing the hydrogen bonding forces of COOH, OH, NH_3^+, and COO^- to become dominant, along with significant chiral recognition of the two molecules.

In the cooling crystallization, generally, the induction temperature is lowered as the cooling rate increased, which implied the crystallization at a high supersaturated solution. It causes the high crystal nucleation and growth, resulting in the incorporation of nonsolute molecules into the crystal lattice. Thereby, in the present study, as the cooling rate increased there occurred an imperfect molecular recognition and an incorporation of L-Phe-D-MA into the diastereomeric crystal of L-Phe-L-MA in the crystallization, resulting in the reduction of the diastereomeric excess, as shown in Figure 8.

The diastereomeric resolution depended significantly on the crystallization temperature in the range of 25−60 °C, as shown in Figure 9. As mentioned above, our solution of L-phenylalanine and mandelic acid was saturated at 75 °C. Thus, the higher crystallization temperature corresponded to the lower supersaturation level for the crystallization. Therefore, the diastereomeric excess of the crystals increased from 63.2% to 69.4% when the crystallization temperature was changed from 25 to 60 °C, indicating that a high crystallization temperature was good for obtaining a high diastereomeric resolution. However, a high crystallization temperature also reduced the recovery of L-MA. For example, the L-MA yield was 79% at 25 °C, yet only 37% at 60 °C. Hence, when selecting the optimal crystallization temperature, both diastereomeric excess and the recovery yield of the diastereomeric crystallization might be compromised. In the present study, a 30−40 °C crystallization temperature was considered as optimum, which produced an diastereomeric resolution of about 66%(de) and a recovery yield of about 70%.

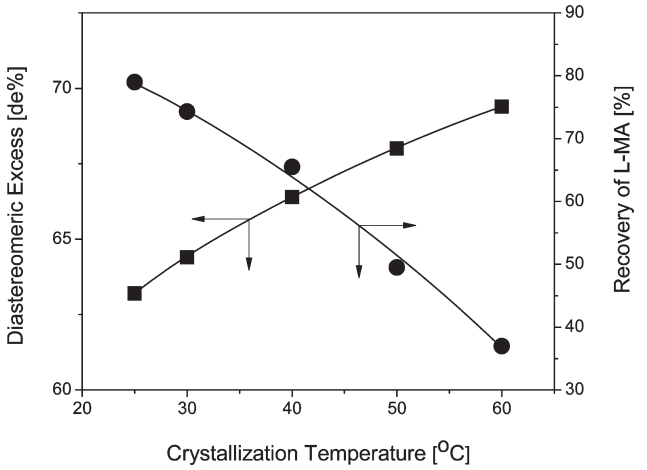

Figure 9. Effect of crystallization temperature on diastereomeric excess of enantio-separation. The molar ratio of MA to L-Phe = 2.0, pH = 3.0, cooling rate = 10 °C/h, agitation speed = 500 rpm.

4. Conclusions

In conclusion, QCM chiral recognition was used as a novel approach to predict the chiral recognizability of a chiral selector for a racemate. An L-Phe-modified QCM sensor was prepared using a two-step assembly procedure. When the chiral recognizability of the L-Phe-modified QCM sensor for L-MA was examined using a VDMA technique, the chiral discrimination factor between L- and D-MA was about 8, suggesting that L-Phe can be a good resolving agent for the resolution of MA. The practical diastereomeric crystallization resolution of a MA racemic compound was then carried out using L-Phe as the resolving agent. The results showed that the diastereomeric crystallization separation of racemate MA using L-Phe as the resolving agent matched well with the QCM chiral recognition results. Consequently, the proposed method offers a simple solution to the challenge of screening resolving agents for diastereomeric crystallization, which until now still uses trial and error. Although this study only examined mandelic acid, this approach also has implications for more general use. However, more extensive validation work is still required. Moreover, because the key step of this approach is to build a proper chiral selector modified surface with recognition sites for a certain enantiomer, special bioconjugate techniques[40] were needed to fulfill this purpose.

Acknowledgment. This work has been financially supported from NRF Research Fund (Korea, 2010-0017993) and the Natural Science Foundation of Guangdong Province, China (9151200501000008).

References

(1) Drayer, D. E. *Clin. Pharmacol. Ther*. **1986**, *40*, 125–133.
(2) Bentley, R. *Chem. Soc. Rev*. **2005**, *34*, 609–624.
(3) Webster, W. S.; Brown-Woodman, P. D.; Ritchie, H. E. *Int. J. Dev. Biol*. **1997**, *41*, 329–335.
(4) Fogassy, E.; Nogradi, M.; Kozma, D.; Egri, G.; Palovics, E.; Kiss, V. *Org. Biomol. Chem*. **2006**, *4*, 3011–3030.
(5) Alegret, C.; Santacana, F.; Riera, A. *J. Org. Chem*. **2007**, *72*, 7688–7692.
(6) Kiau, S.; Discordia, R. P.; Madding, G.; Okuniewicz, F. J.; Rosso, V.; Venit, J. J. *J. Org. Chem*. **2004**, *69*, 4256–4261.
(7) Karamertzanis, P. G.; Price, S. L. *J. Phys. Chem. B* **2005**, *109*, 17134–17150.
(8) Goldberg, S. I. *Origins Life Evol. Biosphere* **2008**, *38*, 149–153.
(9) Trung, T. Q.; Kim, J. M.; Kim, K. H. *Arch. Pharm. Res*. **2006**, *29*, 108–111.
(10) Valente, E. J.; Moore, M. C. *Chirality* **2000**, *12*, 16–25.
(11) Ferrayoli, C. G.; Palacio, M. A.; Bresina, M. F.; Palacios, S. M. *Enantiomer* **2000**, *5*, 289–291.
(12) Marchand, P.; Lefebvre, L.; Querniard, F.; Cardinael, P.; Perez, G.; Counioux, J. J.; Coquerel, G. *Tetrahedron-Asymmetry* **2004**, *15*, 2455–2465.
(13) Martin, A.; Cocero, M. J. *J. Supercrit. Fluids* **2007**, *40*, 67–73.
(14) Sakai, K.; Sakurai, R.; Nohira, H. *Novel Opt. Resolution Technol*. **2007**, *269*, 199–231.
(15) Whitesell, J. K.; Reynolds, D. *J. Org. Chem*. **1983**, *48*, 3548–3551.
(16) Yadav, G. D.; Sivakumar, P. *Biochem. Eng. J*. **2004**, *19*, 101–107.
(17) Zingg, S. P.; Arnett, E. M.; McPhail, A. T.; Bothnerby, A. A.; Gilkerson, W. R. *J. Am. Chem. Soc*. **1988**, *110*, 1565–1580.
(18) Vries, T.; Wynberg, H.; van Echten, E.; Koek, J.; ten Hoeve, W.; Kellogg, R. M.; Broxterman, Q. B.; Minnaard, A.; Kaptein, B.; van der Sluis, S.; Hulshof, L. A.; Kooistra, J. *Angew. Chem., Int. Ed*. **1998**, *37*, 2349–2354.
(19) Vries, T.; Wynberg, H.; van Echten, E.; Koek, J.; ten Hoeve, W.; Kellogg, R. M.; Broxterman, Q. B.; Minnaard, A.; Kaptein, B.; van der Sluis, S.; Hulshof, L. A.; Kooistra, J. *Angew. Chem*. **1998**, *110*, 2491–2496.
(20) Kellogg, R. M.; Nieuwenhuizen, J. W.; Pouwer, K.; Vries, T. R.; Broxterman, Q. B.; Grimbergen, R. F. P; Kaptein, B.; La Crois, R. M.; de Wever, E.; Zwaagstra, K.; van der Laan, A. C. *Synthesis* **2004**, *10*, 1626–1638.
(21) Jacquest, J.; Collet, A.; Wilen, S. H. *Enantiomers, Racemates and Resolutions*; Wiley: New York, 1981.
(22) ten Hoeve, W.; Wynberg, H. *J. Org. Chem*. **1985**, *50*, 4508–4514.
(23) ten Hoeve, W.; Wynberg, H. Eur. Pat. 180,276, 1989; US Pat. 4,814,477, 1989.
(24) Loh, J. S. C.; van Enckevort, W. J. P.; Vlieg, E. *Cryst. Des. Growth* **2006**, *6*, 861–865.
(25) Inomata, T.; Eguchi, H.; Matsumoto, K.; Funahashi, Y.; Ozawa, T.; Masuda, H. *Biosens. Bioelectron*. **2007**, *23*, 751–755.
(26) Weng, W.; Han, J. L.; Chen, Y. Z.; Huang, X. J. *Prog. Chem*. **2007**, *19*, 1820–1825.
(27) Cao, L.; Zhou, X. C.; Li, S. F. Y. *Analyst* **2001**, *126*, 184–188.
(28) Maier, N. M.; Lindner, W. *Anal. Bioanal. Chem*. **2007**, *389*, 377–397.
(29) Guo, W.; Wang, J.; Wang, C.; He, J. Q.; He, X. W.; Cheng, J. P. *Tetrahedron Lett*. **2002**, *43*, 5665–5667.
(30) Kim, W. S.; Lee, H. Y.; Kawai, T.; Kang, H. W.; Muramatsu, H.; Kim, I. H.; Park, K. M.; Chang, S. M.; Kim, J. M. *Sens. Actuat. B* **2008**, *129*, 126–133.
(31) Zhang, S.; Ding, J. J.; Liu, Y.; Kong, J. L.; Hofstetter, O. *Anal. Chem*. **2006**, *78*, 7592–7596.
(32) Guo, H. S.; Kim, J. M.; Kim, S. J.; Chang, S. M.; Kim, W. S. *Langmuir* **2009**, *25*, 648–52.
(33) Kim, W. S.; Kim, S. J.; Park, J. J.; Chang, S. M.; Kim, J. M. *J. Phys. Chem. Solids* **2008**, *69*, 1422–1427.
(34) Guo, H. S.; Kim, J. M.; Chang, S. M.; Kim, W.-S. *J. Nanosci. Nanotechnol*. **2009**, *9*, 2937–2943.
(35) Xu, C. H.; Ng, S. C.; Chan, H. S. O. *Langmuir* **2008**, *24*, 9118–9124.
(36) Paolesse, R.; Monti, D.; La Monica, L.; Venanzi, M.; Froiio, A.; Nardis, S.; Di Natale, C.; Martinelli, E.; D'Amico, A. *Chem.—Eur. J*. **2002**, *8*, 2476–2483.
(37) Nakanishi, T.; Yamakawa, N.; Asahi, T.; Shibata, N.; Ohtani, B.; Osaka, T. *Chirality* **2004**, *16*, S36–S39.
(38) Ng, S. C.; Sun, T.; Chan, H. S. O. *Tetrahedron Lett*. **2002**, *43*, 2863–2866.
(39) Ng, S. C.; Sun, T.; Chan, H. S. O. *Macromol. Symp*. **2003**, *192*, 171–181.
(40) Sauerbrey, G. Z. *Z. Phys*. **1959**, *155*, 206–222.
(41) Tsourkas, A.; Hofstetter, O.; Hofstetter, H.; Weissleder, R.; Josephson, L. *Angew. Chem., Int. Ed*. **2004**, *43*, 2395–2399.
(42) Li, Q. W.; Gao, H.; Wang, Y. M.; Luo, G. A.; Ma, J. *Electroanalysis* **2001**, *13*, 1342–1346.
(43) Yatsimirskii, K. B.; Nemoskalenko, V. V.; Aleshin, V. G.; Bratushko, Y. I.; Moiseenko, E. P. *Chem. Phys. Lett*. **1977**, *52*, 481–484.
(44) Wagner, C. D.; Zatko, D. A.; Raymond, R. H. *Anal. Chem*. **1980**, *52*, 1445–1451.
(45) Okamura, K.; Aoe, K. I.; Hiramatsu, H.; Nishimura, N.; Sato, T.; Hashimoto, K. *Anal. Sci*. **1997**, *13*, 315–317.
(46) Okamura, K.; Aoe, K.; Hiramatsu, H.; Nishimura, N.; Sato, T.; Hashimoto, K. *Analytical Sciences* **1997**, *13*, 315–318.
(47) Nishi, H.; Terabe, S. *J. Chromatogr. A* **1995**, *694*, 245–276.
(48) Ojima, I. *Catalytic Asymmetric Synthesis*; Wiley-VCH: New York, 1993.
(49) Qian, R.; Botsaris, G. *Chem. Eng. Sci*. **1998**, *53*, 1745–1756.
(50) Qin, M.; Bartus, J.; Jaycox, G. D. *Monatsh. fur Chem*. **1995**, *126*, 67–73.
(51) Woiciechowski, K. *Cryst. Res. Technol*. **1999**, *34*, 661–666.
(52) Veintemillas-Verdaguer, S.; Esteban, S. O.; Herrero, M. A. *J. Cryst. Growth* **2007**, *303*, 562–567.